The incorporation efficiency was calculated from Eq. (3) [13];

$$\text{Incorporation efficiency}(\%) = D_e/D_t \times 100 \quad (3)$$

where D_e is the drug amounts recovered in the liposomal fractions and D_t is the drug amounts in applied liposomes to a gel column, respectively.

2.9. Statistical analysis

Statistical comparisons were performed by both analysis of variance and Tukey multiple comparison test. $P<0.05$ was considered to be indicative of statistical significance.

3. Results

3.1. Physicochemical properties of PLS and Pal-PLS

The structures and physicochemical properties of the compounds tested in the present investigation are summarized in Table 1. The lipophilicity of Pal-PLS was confirmed by measuring $\log k'_0$ in the HPLC system. Pal-PLS showed higher lipophilicity compared with PLS.

Table 3
Incorporation efficiency of PLS and Pal-PLS into various liposomes in gel filtration

Entry	Drug	Lipid composition (molar ratio)	Incorporation efficiency (%)
1	PLS	EggPC:Chol (3:2)	0.1 ± 0.1
2	PLS	EggPC:Chol:DSPE-PEG 2000 (3:2:0.05)	1.2 ± 0.8
3	PLS	EggPC:Chol:DSPE-PEG 5000 (3:2:0.05)	2.4 ± 2.1
4	PLS	DSPC:Chol (3:2)	1.7 ± 1.0
5	PLS	DSPC:Chol:DSPE-PEG 2000 (3:2:0.05)	1.9 ± 1.5
6	PLS	DSPC:Chol:DSPE-PEG 5000 (3:2:0.05)	4.3 ± 3.0
7	Pal-PLS	EggPC:Chol (3:2)	71.3 ± 3.5
8	Pal-PLS	EggPC:Chol:DSPE-PEG 2000 (3:2:0.05)	82.7 ± 9.8
9	Pal-PLS	EggPC:Chol:DSPE-PEG 5000 (3:2:0.05)	88.9 ± 4.1
10	Pal-PLS	DSPC:Chol (3:2)	91.2 ± 7.1
11	Pal-PLS	DSPC:Chol:DSPE-PEG 2000 (3:2:0.05)	90.2 ± 1.8
12	Pal-PLS	DSPC:Chol:DSPE-PEG 5000 (3:2:0.05)	91.9 ± 3.8

Each value represents the average ± S.D. of at least three experiments.

Table 4
The effect of plasma on incorporation efficiency of Pal-PLS into various liposomes in gel filtration

Entry	Drug	Lipid composition (molar ratio)	Incorporation efficiency (%)
7	Pal-PLS	EggPC:Chol (3:2)	46.0 ± 5.5
8	Pal-PLS	EggPC:Chol:DSPE-PEG 2000 (3:2:0.05)	83.1 ± 3.6*
9	Pal-PLS	EggPC:Chol:DSPE-PEG 5000 (3:2:0.05)	83.0 ± 1.0*
10	Pal-PLS	DSPC:Chol (3:2)	88.4 ± 7.2*
11	Pal-PLS	DSPC:Chol:DSPE-PEG 2000 (3:2:0.05)	87.4 ± 6.8*
12	Pal-PLS	DSPC:Chol:DSPE-PEG 5000 (3:2:0.05)	88.0 ± 2.9*

Each value represents the average ± S.D. of at least three experiments.

* Significantly different from Entry 7 ($P<0.05$, Tukey multiple comparison test).

3.2. Ultrafiltration

The trapping efficiency of PLS and Pal-PLS by various liposomes was calculated after ultrafiltration and is shown in Table 2. More than 80% of not only PLS but also Pal-PLS were trapped by the liposomes consisting of various lipids. In the preliminary experiments, it was confirmed that there was little adhesion of drugs with ultrafiltrated membrane.

3.3. Gel filtration

The typical gel filtration profiles for EggPC/Chol and DSPC/Chol liposomes incorporating PLS and Pal-PLS are shown in Fig. 1. The first and second peaks of FD-4 are considered to be the incorporated drug into liposomes (liposomal fraction) and non-incorporated drug (free fraction), respectively. PLS was mostly existed in the free fraction, although Pal-PLS was mostly retained in liposomal fraction.

The incorporation efficiencies of PLS and Pal-PLS into various liposomes were calculated from gel filtration profiles and are summarized in Table 3. Although PLS showed high trapping efficiency by all liposomes after ultrafiltration, the low incorporation efficiency of PLS into all liposomes was observed

in the gel filtration. On the other hand, Pal-PLS showed high incorporation into all liposomes not only in ultrafiltration but also in gel filtration.

3.4. Effect of plasma on Pal-PLS retention in liposomes

The effect of plasma on Pal-PLS retention in the liposomes was evaluated by gel filtration. After liposomes were incubated for 1 min with rat plasma, they were applied to a gel column and eluted with PBS. The incorporation efficiency of Pal-PLS was calculated from gel filtration profiles and is summarized in Table 4. The incorporation efficiency of Pal-PLS into EggPC/Chol liposomes reduced to approximately 65% after their incubation with plasma compared with the value without plasma. On the other hand, approximately 97% incorporation of Pal-PLS was observed in DSPC/Chol liposomes after their incubation with plasma. Addition of DSPE-PEG 2000 or DSPE-PEG 5000 to EggPC/Chol liposomes also showed high incorporation of Pal-PLS after their incubation with plasma.

4. Discussion

Recently, drug delivery systems using liposomes as drug carriers have been well studied to achieve controlled and site-specific delivery of drugs [14–17]. Liposomes have various advantages as a drug carrier: biodegradability, low in vivo toxicity, and encapsulation of hydrophilic, lipophilic and amphipathic drugs. Introduction of thermosensitive lipid to liposomes [14] and modification of the liposomal membrane by galactose [15] have been reported to be useful for achievement of further drug targeting. In systemic circulation, however, drugs incorporated into liposomes were diluted by blood, followed by the interaction with plasma components [18–20]; consequently, incorporated drugs were rapidly released from liposomes [21].

In liposomes, lipophilic drugs were retained in the liposomal lipid bilayer, although water-soluble drugs were retained inside the aqueous phase [22]. We newly synthesized Pal-PLS as a lipophilic derivative of PLS to increase its affinity to lipid bilayer. The initial step in producing biological responses to administered corticosteroids is the diffusion of unbound drug from plasma into cells for interaction with cytosolic receptors. Pal-PLS might be extremely less active than PLS because the chemically modified part of Pal-PLS seems to be important for its nuclear receptor binding. On the other hand, Pal-PLS was rapidly biodegraded to PLS in the presence of not only rat liver homogenate but also rat plasma in the preliminary experiments (data not shown). Therefore, it is considered that Pal-PLS released from liposomes must convert to PLS rapidly under biological condition and show therapeutic activity.

The retention property of PLS and Pal-PLS in various liposomes was investigated by ultrafiltration and gel filtration. PLS is lipophilic drug and its liposomes showed an increased therapeutic efficiency in IgA nephropathy model mice compared with PLS alone owing to enhancement of kidney delivery [2]. Actually, PLS was well incorporated into various liposomes as the results from ultrafiltration (Table 2). Ultrafiltration method could measure trapping efficiency of liposomes simply and immediately after their preparation. The incorporation of PLS into the liposomes, however, was dramatically decreased in the gel filtration (Table 3). The amounts of FD-4, hydrophilic marker, in liposomal fractions containing PLS had no significant difference from those in liposomal fractions containing Pal-PLS. This result indicated that PLS was released from liposomes by a dilution with elution medium without the collapse of liposomes in the process of gel filtration. As the results in the gel filtration, most of PLS must be released from any liposomes by dilution with blood circulation after their administration in vivo.

On the other hand, Pal-PLS showed highly incorporation efficiency not only in ultrafiltration but also in gel filtration (Table 3). It is demonstrated that the enhanced lipophilicity of drug itself is more important to improve the drug retention in liposomes compared with pharmaceutical approach using special lipids.

It is well known that liposomes were largely influenced by biological component under in vivo condition [23]. Therefore, the influence of rat plasma on retention of Pal-PLS in the liposomes was determined by gel filtration. As the results, rat plasma decreased incorporation efficiency of Pal-PLS into EggPC/Chol liposomes. DSPC/Chol liposomes

showed high incorporation efficiency of Pal-PLS even after their incubation with rat plasma (Table 4). DSPC and EggPC have been chosen as a typical lipid for preparing the liposomes that are commonly used as drug delivery [24,25]. Silvander et al. [24] reported that DSPC/Chol liposomes highly incorporated various fluorescent dyes compared with EggPC/Chol liposomes. Senior et al. [26] also demonstrated that DSPC/Chol liposomes showed longer half-lives than EggPC/Chol liposomes after their intravenous injection to mice. It is recognized that liposomes composed of unsaturated lipids with low phase transition temperatures display lower stability towards leakage than saturated analogues with higher phase transitions. In the experiments of the monolayer interactions of phospholipids and Chol, Demel et al. [27] reported that saturated phospholipids such as DSPC could condense with Chol partially by Van der Waals interaction. The stable retention of Pal-PLS in the DSPC/Chol liposomes after their incubation with rat plasma may be explained by the condensation effect and the high phase transition temperature of DSPC.

Surface modification of liposomes with the hydrophilic polymer PEG has provided a major advance in drug delivery applications due to the ability of this polymer to reduce protein binding and plasma elimination of liposomes [28]. The medical utility of these long circulation liposomes is displayed by the fact that several liposomal drugs are on the market or in late stage clinical trials [29,30]. In fact, PEGylation using DSPE-PEG 2000 and DSPE-PEG 5000 induced the low incorporation efficiency of EggPC/Chol liposomes after their incubation with rat plasma (Table 4). Addition of PEG-lipids on liposomes formed hydrophilic outer layer, and the hydrophilic surface protect liposomes from plasma components binding and subsequent mononuclear phagocytic system uptake [28]. It is valuable to note that not only water-soluble drug but also lipophilic drug such as Pal-PLS that may be inserted into liposomal lipid bilayer was stably retained in PEG-modified liposomes in the presence of plasma.

The activity of liposomal corticosteroids should depend on the various procedures such as drug release from liposomes in blood, uptake of liposome by target cells, and drug release from liposomes in cytoplasm. Strong retention of drugs into liposomes can not always improve its pharmacokinetics and activity. Optimization of retention and release of drugs in liposomes is considered to be very important for therapeutic success. Our data indicated that adjustment of drug lipophilicity and lipid compositions including PEG-lipids is a promising approach to prepare adequate liposomes of PLS. On the other hand, gel filtration method could be useful for liposomal formulations to simultaneously evaluate both their dilution by blood circulation and interaction with biological components under in vivo condition.

5. Conclusion

We systemically examined about the drug retention from various liposomes in the ultrafiltration and gel filtration. The enhanced lipophilicity of drug was more important to improve the drug retention in liposomes than lipid compositions of liposomes. The release of lipophilic derivative from the liposomes by plasma was efficiently protected by selection of lipids and PEGylation.

Acknowledgements

This work was supported in part by a Grant-in-Aid for Scientific Research from the Ministry of Education, Culture, Sports, Science, and Technology, Japan. The authors thank Naomi Takada for technical assistance.

References

[1] C.H. Robert, M. Ferid, in: P.B. Molinoff, R.W. Ruddon (Eds.), Goodman and Gilman's The Pharmacological Basis of Therapeutics, McGraw-Hill, New York, 1996, pp. 1459–1489.
[2] J. Liao, K. Hayashi, S. Horikoshi, H. Ushijima, J. Kimura, Y. Tomino, Effect of steroid-liposome on immunohistopathology of IgA nephropathy in ddY mice, Nephron 89 (2001) 194–200.
[3] E.V. Mishina, J. Binder, J.W. Kupiec-Weglinski, W.J. Jusko, Effect of liposomal methylprednisolone on heart allograft survival and immune function in rats, J. Pharmacol. Exp. Ther. 271 (1994) 868–874.
[4] S.M. Moghimi, H.M. Patel, Serum opsonins and phagocytosis of saturated and unsaturated phospholipid liposomes, Biochim. Biophys. Acta 984 (1989) 384–387.
[5] N. Shibuya-Fujiwara, F. Hirayama, Y. Ogata, H. Ikeda, K. Ikebuchi, Phagocytosis in vitro of polyethylene glycol-modi-

fied liposome-encapsulated hemoglobin by human peripheral blood monocytes plus macrophages through scavenger receptors, Life Sci. 70 (2001) 291–300.
[6] T.M. Allen, C. Hansen, F. Martin, C. Redemann, A. Yau-Young, Liposomes containing synthetic lipid derivatives of poly(ethylene glycol) show prolonged circulation half-lives in vivo, Biochim. Biophys. Acta 1066 (1991) 29–36.
[7] M.C. Woodle, K.K. Matthay, M.S. Newman, J.E. Hidayat, L.R. Collins, C. Redemann, F.J. Martin, D. Papahadjopoulos, Versatility in lipid compositions showing prolonged circulation with sterically stabilized liposomes, Biochim. Biophys. Acta 1105 (1992) 193–200.
[8] H. Sasaki, Y. Takakura, M. Hashida, T. Kimura, H. Sezaki, Antitumor activity of lipophilic prodrugs of mitomycin C entrapped in liposome or O/W emulsion, J. Pharmacobiodyn. 7 (1984) 120–130.
[9] S. Kawakami, K. Yamamura, T. Mukai, K. Nishida, J. Nakamura, T. Sakaeda, M. Nakashima, H. Sasaki, Sustained ocular delivery of tilisolol to rabbits after topical administration or intravitreal injection of lipophilic prodrug incorporated in liposomes, J. Pharm. Pharmacol. 53 (2001) 1157–1161.
[10] T. Yamana, A. Tsuji, E. Miyamoto, O. Kubo, Novel method for determination of partition coefficients of penicillins and cephalosporins by high-pressure liquid chromatography, J. Pharm. Sci. 66 (1977) 747–749.
[11] C. Huang, Studies on phosphatidylcholine vesicles. Formation and physical characteristics, Biochemistry 8 (1969) 344–352.
[12] K. Taniguchi, N. Yamazawa, K. Itakura, K. Morisaki, S. Hayashi, Partition characteristics and retention of anti-inflammatory steroids in liposomal ophthalmic preparations, Chem. Pharm. Bull. 35 (1987) 1214–1222.
[13] Y. Tokunaga, T. Iwasa, J. Fujisaki, S. Sawai, A. Kagayama, Liposomal sustained-release delivery systems for intravenous injection: I. Physicochemical and biological properties of newly synthesized lipophilic derivatives of mitomycin C, Chem. Pharm. Bull. 36 (1988) 3060–3069.
[14] S. Unezaki, K. Maruyama, N. Takahashi, M. Koyama, T. Yuda, A. Suginaka, M. Iwatsuru, Enhanced delivery and antitumor activity of doxorubicin using long-circulating thermosensitive liposomes containing amphipathic polyethylene glycol in combination with local hyperthermia, Pharm. Res. 11 (1994) 1180–1185.
[15] S. Kawakami, C. Munakata, S. Fumoto, F. Yamashita, M. Hashida, Targeted delivery of prostaglandin E_1 to hepatocytes using galactosylated liposomes, J. Drug Target. 8 (2000) 137–142.
[16] K. Moribe, K. Maruyama, Pharmaceutical design of the liposomal antimicrobial agents for infectious disease, Curr. Pharm. Des. 8 (2002) 441–454.
[17] H. Iinuma, K. Maruyama, K. Okinaga, K. Sasaki, T. Sekine, O. Ishida, N. Ogiwara, K. Johkura, Y. Yonemura, Intracellular targeting therapy of cisplatin-encapsulated transferrin-polyethylene glycol liposome on peritoneal dissemination of gastric cancer, Int. J. Cancer 99 (2002) 130–137.
[18] C. Kirby, J. Clarke, G. Gregoriadis, Cholesterol content of small unilamellar liposomes controls phospholipid loss to high density lipoproteins in the presence of serum, FEBS Lett. 111 (1980) 324–328.
[19] J. Senior, G. Gregoriadis, Stability of small unilamellar liposomes in serum and clearance from the circulation: the effect of the phospholipid and cholesterol components, Life Sci. 30 (1982) 2123–2136.
[20] F. Frézard, C. Santaella, P. Vierling, J.G. Riess, Permeability and stability in buffer and in human serum of fluorinated phospholipid-based liposomes, Biochim. Biophys. Acta 1192 (1994) 61–70.
[21] T. Takino, C. Nakajima, Y. Takakura, H. Sezaki, M. Hashida, Controlled biodistribution of highly lipophilic drugs with various parenteral formulations, J. Drug Target. 1 (1993) 117–124.
[22] C.G. Knight, in: C.G. Knight (Ed.), Liposomes from Physical Structure to Therapeutic Application, Elsevier/North-Holland Biomedical Press, Amsterdam, 1981, pp. 381–390.
[23] T. Ishida, H. Harashima, H. Kiwada, Liposome clearance, Biosci. Rep. 22 (2002) 197–224.
[24] M. Silvander, M. Johnsson, K. Edwards, Effects of PEG-lipids on permeability of phosphatidylcholine/cholesterol liposomes in buffer and in human serum, Chem. Phys. Lipids 97 (1998) 15–26.
[25] E. Ruel-Gariépy, G. Leclair, P. Hidgen, A. Gupta, J.C. Leroux, Thermosensitive chitosan-based hydrogel containing liposomes for the delivery of hydrophilic molecules, J. Control. Release 82 (2002) 373–383.
[26] J. Senior, J.C. Crawley, G. Gregoriadis, Tissue distribution of liposomes exhibiting long half-lives in the circulation after intravenous injection, Biochim. Biophys. Acta 839 (1985) 1–8.
[27] R.A. Demel, L.L.M. Van Deenen, B.A. Pethica, Monolayer interactions of phospholipids and cholesterol, Biochim. Biophys. Acta 135 (1967) 11–19.
[28] J. Senior, C. Delgado, D. Fisher, C. Tilcock, G. Gregoriadis, Influence of surface hydrophilicity of liposomes on their interaction with plasma protein and clearance from the circulation: studies with poly(ethylene glycol)-coated vesicles, Biochim. Biophys. Acta 1062 (1991) 77–82.
[29] M.C. Woodle, Sterically stabilized liposome therapeutics, Adv. Drug Deliv. Rev. 16 (1995) 249–265.
[30] H. Ruey-Long, T. Yun-Long, Phase I and pharmacokinetic study of a stable, polyethylene-glycolated liposomal doxorubicin in patients with solid tumors, Cancer 91 (2001) 1826–1833.

Ocular Pharmacokinetic/ Pharmacodynamic Modeling for Bunazosin After Instillation into Rabbits

Koji Sakanaka,[1,2] Kouichi Kawazu,[2] Masahide Tomonari,[1] Takashi Kitahara,[1] Mikiro Nakashima,[1] Shigeru Kawakami,[3] Koyo Nishida,[3] Junzo Nakamura,[3] and Hitoshi Sasaki[1,4]

Received September 3, 2003; accepted January 29, 2004

Purpose. To develop a pharmacokinetic/pharmacodynamic (PK/PD) model for an α_1-blocker (bunazosin) after instillation. The PK/PD model can predict both the drug concentrations in various ocular tissues and the hypotensive effect.

Methods. Bunazosin concentrations were determined with High Performance Liquid Chromatography (HPLC) in tear fluid, the aqueous humor, cornea, and iris-ciliary body after instillation or ocular injection into the anterior chamber in rabbits. After instillation of bunazosin in rabbits, intraocular pressure (IOP) was also determined with a pneumatic tonometer. The PK/PD parameters were estimated by fitting the concentration-time profiles and the hypotensive effect-time profiles to the developed PK/PD models using the MULTI (RUNGE) program.

Results. On the basis of the concentration-time profiles of bunazosin, a PK model, including seven compartments, was developed for examining the behavior of bunazosin after instillation. Then, two PK/PD models for hypotensive effect of bunazosin were developed using an indirect response (model A) and the relationship between IOP and aqueous humor flow (model B). These models well described the concentration-time profiles and hypotensive effect-time profiles of bunazosin after instillation.

Conclusions. This study is the first trial to develop a PK/PD model for an antiglaucoma agent using an indirect response and the relationship between IOP and aqueous humor flow.

KEY WORDS: bunazosin; eye; indirect response; intraocular pressure; pharmacokinetic/pharmacodynamic model.

INTRODUCTION

Upon instillation of an ophthalmic drug, most of the instilled drug is rapidly eliminated from the precorneal area due to drainage through the nasolacrimal duct and dilution by tear turnover (1). These physiological complexities have interfered with the development of pharmacokinetic (PK) models for ophthalmic agents. Logical use of ophthalmic drugs based on a knowledge of pharmacokinetics is important for effective medication. In a previous report, we successfully developed an ocular PK model that accounted for the corneal diffusion process to predict the behavior of instilled β-blockers (2).

On the other hand, the pharmacodynamics of an instilled drug are more important than the pharmacokinetics in the design of an appropriate dosage form and regimen to achieve the desired therapeutic effect on patients. However, there have been few reports of ocular pharmacokinetic/pharmacodynamic (PK/PD) models for ophthalmic drugs after instillation. Especially, the pharmacokinetics of antiglaucoma agents in ocular tissues and their relationship to the corresponding intraocular pressure (IOP) has never been thoroughly investigated.

In the current study, we newly developed an ocular PK/PD model that enabled us to predict both the drug concentrations in ocular tissues and the IOP after instillation of bunazosin in rabbits. Bunazosin (α_1-blocker) is commercially available as a new antiglaucoma agent.

MATERIALS AND METHODS

Animals

Male Nippon albino rabbits (2.0–3.0 kg) were individually housed in cages in an air-conditioned room and maintained on a standard laboratory diet (ORC4, Oriental Yeast Co., Ltd., Tokyo, Japan). The rabbits had free access to water and were maintained in a 12-h light-dark cycle (lights on at 7:00 AM, and lights off at 7:00 PM). All experiments in the current study conformed to the"Principles of Laboratory Animal Care"(NIH Publication No. 85-23, revised 1985).

Materials

Bunazosin hydrochloride was kindly supplied from Santen Pharmaceutical Co., Ltd. (Osaka, Japan). Prazosin hydrochloride was purchased from Wako Pure Chemical Industries, Ltd. (Osaka, Japan). All other chemicals of reagent grade were obtained from Nacalai Tesque Inc. (Kyoto, Japan). The drug solution was prepared with pH 7.4 phosphate-buffered saline (PBS).

Drug Disposition After Instillation

Unanesthetized rabbits were placed in restraint boxes. Twenty-five μl of drug solution (bunazosin: 0.1%) were carefully instilled with a micropipette (Gilson Medical Electronics, Villiers-le-Bel, France) into the middle of the lower conjunctival eye sac. At the appropriate time after instillation, tear fluid (0.5 μl) was collected in glass capillary (EM minicaps, Hirschmann Laborgerate, Eberstadt, Germany) from the middle of a lower marginal tear strip and diluted with 50 μl of acetonitrile.

Under the same conditions, the rabbits were sacrificed by an overdose of sodium pentobarbital at the appropriate time after drug instillation. After thoroughly rinsing the corneal and conjunctival surfaces with 0.9% NaCl and blotting them dry, the aqueous humor was aspirated from the anterior chamber using a 1.0-ml disposable syringe with a 27-gauge needle. The cornea and iris-ciliary body were dissected with a surgical knife. The samples were submitted to an HPLC assay.

[1] Department of Hospital Pharmacy, Nagasaki University School of Medicine, Nagasaki 852-8501, Japan.
[2] Santen Pharmaceutical Co., Ltd., Nara Research and Development Center, Ikoma-shi 630-0101, Japan.
[3] Graduate School of Biomedical Sciences, Nagasaki University, Nagasaki 852-8521, Japan.
[4] To whom correspondence should be addressed. (e-mail sasaki@net.nagasaki-u.ac.jp)

Drug Disposition After Ocular Injection

Unanesthetized rabbits were placed in restraint boxes. About 10 min before the administration of the drug, the eyes were anesthetized locally with 0.4% oxybuprocaine hydrochloride. One microliter of drug solution (bunazosin: 0.01%) was injected into the anterior chamber using a microsyringe fitted with a 30-gauge needle. After injection, the needle was carefully removed to prevent leaks of drug solution. The protocol for sampling the aqueous humor and other tissues was as described above. The samples were then submitted for an HPLC assay.

Drug Determination

The tear fluid samples for bunazosin were centrifuged at 8000*g* for 10 min and the supernatants (10–30 μl) were mixed with water (60 μl) after appropriate dilution with acetonitrile. The samples (50 μl) were injected into an HPLC system. The drug concentrations were determined with an external standard.

The aqueous humor samples of bunazosin were mixed with acetonitrile (1 ml) containing an internal standard (20 nM prazosin hydrochloride). The cornea and iris-ciliary body were homogenized with acetonitrile (1 ml) containing an internal standard (20 nM prazosin hydrochloride) on ice. These mixtures were centrifuged at 8000*g* for 5 min, and the supernatants (100 μl) were diluted with 200 μl of water. The samples (50 μl) were then injected into an HPLC system.

The HPLC system (LC-10AD, Shimadzu Co., Ltd., Kyoto, Japan) was used in the reversed-phase mode for the assay. The stationary phase used was a TSKgel ODS-80T_M packed column (250 mm length × 4.6 mm i.d., Tosoh Inc., Tokyo, Japan). A mixture of acetonitrile and 66 mM NaH_2PO_4 (3:7, v/v) was used for the mobile phase with a flow rate of 0.6 ml/min (for tear samples) or 0.8 ml/min (for ocular tissue samples). Retention of the drug was monitored with a spectrofluorometric detector (RF-10A, Shimadzu Co., Ltd.; excitation wavelength 350 nm, emission wavelength 405 nm).

Measurement of IOP

Unanesthetized rabbits trained enough to be handled were placed in restraint boxes. Twenty-five microliters of drug solution (bunazosin: 0.002%, 0.01%, and 0.1%) were carefully instilled into the rabbits' eyes. The control group received 25 μl of PBS. One drop of 0.4% oxybuprocaine hydrochloride was instilled into both eyes prior to IOP measurements. IOP was determined using a pneumatic tonometer (Modeling 30 Classic Pneumatonometer, Mentor Co., Ltd., Santa Barbara, CA, USA).

Data Analysis

The concentration-time profiles for bunazosin in the tear fluid (Fig. 1) were analyzed by a two-compartment model. The concentration (C_T) at time t is expressed as follows:

$$C_T = A \cdot e^{-\alpha \cdot t} + B \cdot e^{-\beta \cdot t} \quad (1)$$

Hybrid parameters, A, B, α, and β, are defined as $\alpha + \beta = K_{TR1} + K_{R1T} + K_{Te}$, $\alpha \cdot \beta = K_{R1T} \cdot K_{Te}$ and $(A \cdot \alpha + B \cdot \beta)/(A + B) = K_{R1T}$. The parameters K_{TR1} and K_{R1T} are the transfer rate constants between the tear fluid and reservoir-1 (Res. 1), and K_{Te} is the elimination rate constant from the tear fluid. The parameters were estimated from the tear fluid concentrations after instillation of bunazosin using MULTI, a nonlinear least-squares computer program (3).

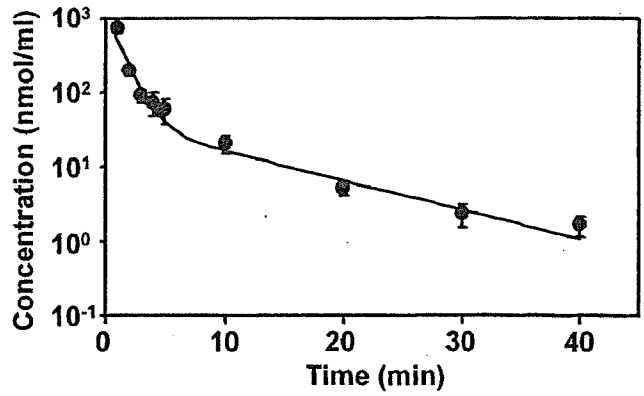

Fig. 1. Concentration of bunazosin in the tear fluid after instillation. (●) Experimental data and (—) fitting line. Each point represents the mean ± SE of at least six experiments.

The ocular behaviors of bunazosin after instillation and injection into the anterior chamber (Figs. 2 and 3) were analyzed by the PK model (Fig. 4) in which the cornea was considered to be divided into two subcompartments, one to represent the epithelium and the other to represent the stroma. Based on this model, the differential equations of drug amounts in the corneal epithelium (X_{CE}), the corneal stroma (X_{CS}), the aqueous humor (X_A), the iris-ciliary body (X_I), and Res. 2 (X_{R2}) can be expressed as follows:

$$\frac{dX_{CE}}{dt} = K_{TC} \cdot X_T - K_{ES} \cdot X_{CE} \quad (2)$$

$$\frac{dX_{CS}}{dt} = K_{ES} \cdot X_{CE} + K_{AC} \cdot X_A - K_{CA} \cdot X_{CS} \quad (3)$$

$$\frac{dX_A}{dt} = K_{CA} \cdot X_{CS} + K_{R2A} \cdot X_{R2} - (K_{AC} + K_{AR2} + K_{AI} + K_{Ae1} + K_{Ae2}) \cdot X_A \quad (4)$$

$$\frac{dX_I}{dt} = K_{AI} \cdot X_A - K_{Ie} \cdot X_I \quad (5)$$

$$\frac{dX_{R2}}{dt} = K_{AR2} \cdot X_A - K_{R2A} \cdot X_{R2} \quad (6)$$

where X_T is drug amount in the tear fluid, K_{TC} is the transfer rate constant from the tear fluid to the corneal epithelium, K_{ES} is the transfer rate constant from the corneal epithelium to the corneal stroma, K_{AI} is the transfer rate constant from the aqueous humor to the iris-ciliary body, K_{CA} and K_{AC} are the transfer rate constants between the corneal stroma and the aqueous humor, K_{AR2} and K_{R2A} are the transfer rate constants between the aqueous humor and Res. 2, K_{Ie} is the elimination rate constant from the iris-ciliary body, and K_{Ae1} and K_{Ae2} are elimination rate constants from the aqueous humor by aqueous humor flow and other routes, respectively. The value of K_{Ae1} was obtained from the data reported by Sakurai *et al.* (4). The PK parameters were estimated from the drug amount-time profiles in the ocular tissues after instilla-

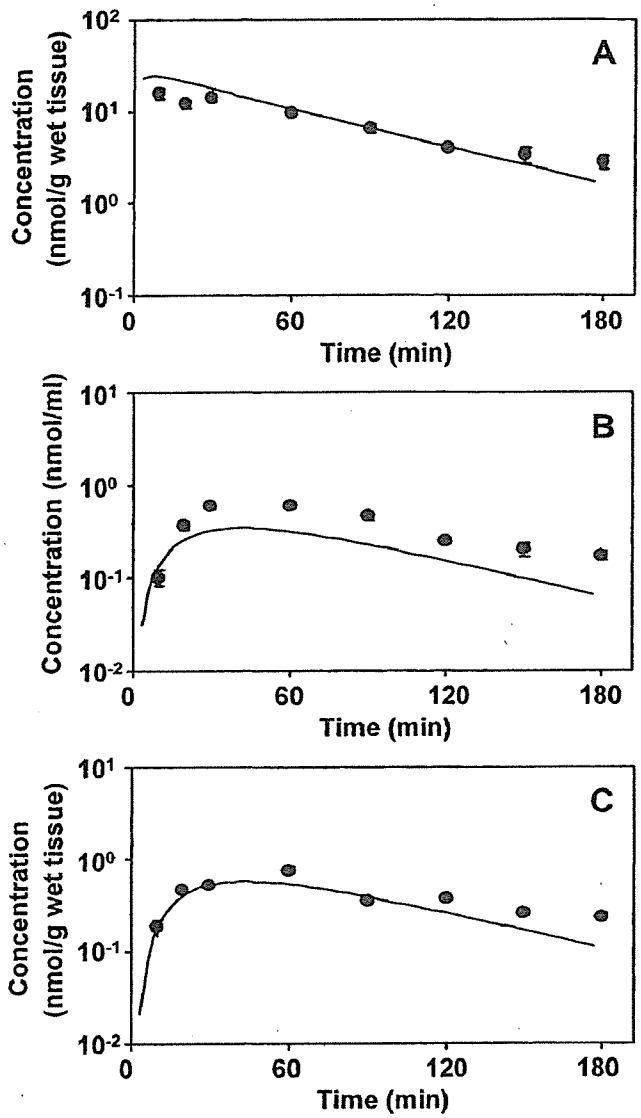

Fig. 2. Concentration of bunazosin in the (A) cornea, (B) aqueous humor, and (C) iris-ciliary body after instillation. (●) Experimental data and (—) fitting line. Each point represents the mean ± SE of at least three experiments.

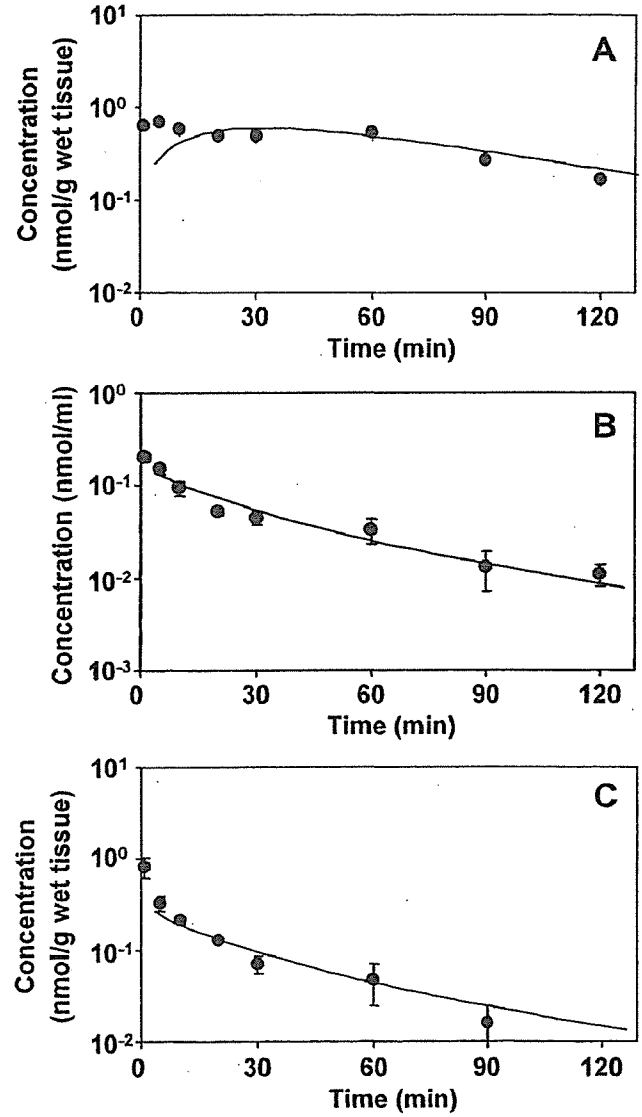

Fig. 3. Concentration of bunazosin in the (A) cornea, (B) aqueous humor, and (C) iris-ciliary body after injection into the anterior chamber. (●) Experimental data and (—) fitting line. Each point represents the mean ± SE of at least three experiments.

tion and injection. The estimations were carried out by using MULTI (RUNGE), a nonlinear least-squares computer program based on the Runge-Kutta-Gill method (5).

Based on reports that bunazosin reduces IOP by increasing outflow of aqueous humor (6,7), the hypotensive effect-time profiles after instillation (Fig. 5) were analyzed by the PK/PD model using an indirect response (Fig. 6A) (8). The model represents a general approach where the rate of change in response is controlled by a zero-order process (zero-order rate constant K_{in}) for production of the response and a first-order process (first-order rate constant K_{out}) for loss of the response. In the indirect response modeling, IOP is produced at zero-order, and IOP loss is indirectly controlled by drug concentrations in the aqueous humor (C_A) according to an E_{max} model, which can be related to receptor theory. The differential equation of IOP can be expressed as follows:

$$\frac{dIOP}{dt} = K_{inA} - K_{outA} \cdot \left(1 + \frac{E_{maxA} \cdot C_A}{EC_{50A} + C_A}\right) \cdot IOP \qquad (7)$$

where K_{inA} is the zero-order rate constant for IOP production, and K_{outA} is the first-order rate constant for IOP loss. It is assumed that K_{inA} and K_{outA} fully account for production and loss of the IOP. E_{maxA} is the maximum effect attributed to the drug, and EC_{50A} is the drug concentration producing 50% of the maximum effect. C_A is defined as $C_A = X_A/V_A$. The aqueous humor volume V_A is obtained from the data reported by Conrad and Robinson (9). The PD parameters were estimated from the hypotensive effect-time profiles after instillation. The estimations were carried out using MULTI (RUNGE).

On the other hand, the hypotensive effect-time profiles after instillation (Fig. 5) were also analyzed by another PK/PD model considering aqueous humor flow (Fig. 6B). This

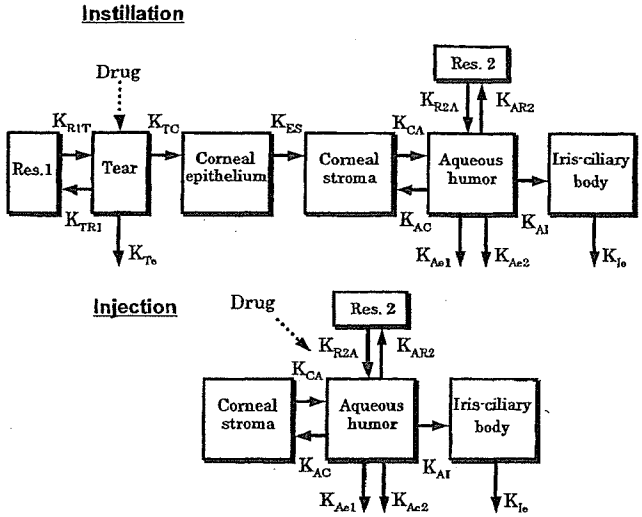

Fig. 4. Pharmacokinetic models for bunazosin in the precorneal area and other tissues after instillation, and after injection into the anterior chamber.

model includes an equilibrium of the aqueous humor flow (F_{in}) to the aqueous humor flow (F_{us}), with trabecular outflow (F_{tra}). F_{tra} expressed as follows:

$$F_{tra} = C_{of}(IOP - P_V) \tag{8}$$

where P_V is the episcleral venous pressure and C_{of} is the outflow facility. Based on these relationships, the IOP was expressed by aqueous humor flow as follows (10):

$$IOP = P_V + \frac{F_{in} - F_{us}}{C_{of}} \tag{9}$$

As bunazosin reduces IOP by increasing uveoscleral outflow (7), the differential equation of IOP after instillation of bunazosin can be expressed as follows:

$$\frac{dIOP}{dt} = -\frac{dF_{us}}{dt} \cdot \frac{1}{C_{of}} \tag{10}$$

In indirect response modeling, F_{us} is indirectly controlled by drug concentrations in the aqueous humor (C_A) according to the E_{max} model. Bunazosin is considered to be a suppressing biological factor, which reduces F_{us} via the α_1-receptor (11). Therefore, the differential equation of F_{us} can be expressed as follows:

$$\frac{dF_{us}}{dt} = K_{inB} - K_{outB} \cdot \left(1 - \frac{E_{maxB} \cdot C_A}{EC_{50B} + C_A}\right) \cdot F_{us} \tag{11}$$

where K_{inB} is the zero-order rate constant for production of F_{us}, and K_{outB} is the first-order rate constant for loss of F_{us}. It is assumed that K_{inB} and K_{outB} fully account for production and loss of the F_{us}. E_{maxB} is the maximum effect attributed to the drug, and EC_{50B} is the drug concentration producing 50% of the maximum effect.

When Eq. 9 and Eq. 11 were substituted in Eq. 10, we obtained the equation for the PK/PD model considering the relationship between IOP and aqueous humor flow as follows:

$$\frac{dIOP}{dt} = -\left\{K_{inB} - K_{outB} \cdot \left(1 - \frac{E_{maxB} \cdot C_A}{EC_{50B} + C_A}\right) \cdot [F_{in} - C_{of} \cdot (IOP - P_V)]\right\} \cdot \frac{1}{C_{of}} \tag{12}$$

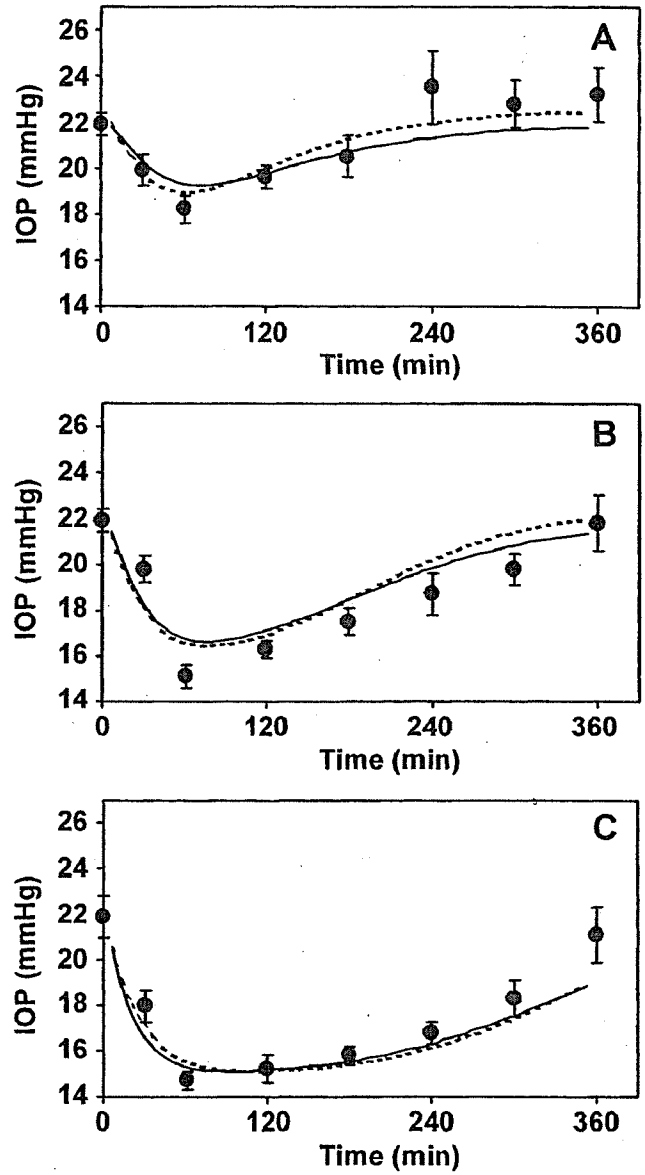

Fig. 5. Intraocular pressures after instillation of bunazosin in rabbits. (A) 0.002%, (B) 0.01%, (C) 0.1%. (●) Experimental data revised by control, (—) fitting line for the indirect response model, (- - -) fitting line for the aqueous humor flow model. Each point represents the mean ± SE of at least 10 experiments.

Physiological parameters P_V, F_{in}, and C_{of} were obtained from the data reported by Sakurai *et al.* (4). PD parameters K_{inB}, K_{outB}, E_{maxB}, and EC_{50B} were estimated from the hypotensive effect-time profiles after instillation of bunazosin. The estimations were carried out using MULTI (RUNGE).

RESULTS

The concentration-time profiles of bunazosin in the ocular tissues were determined after its instillation into the rabbits' eyes. Figure 1 shows the concentrations of bunazosin in the tear fluid. The profile showed a biexponential curve. The

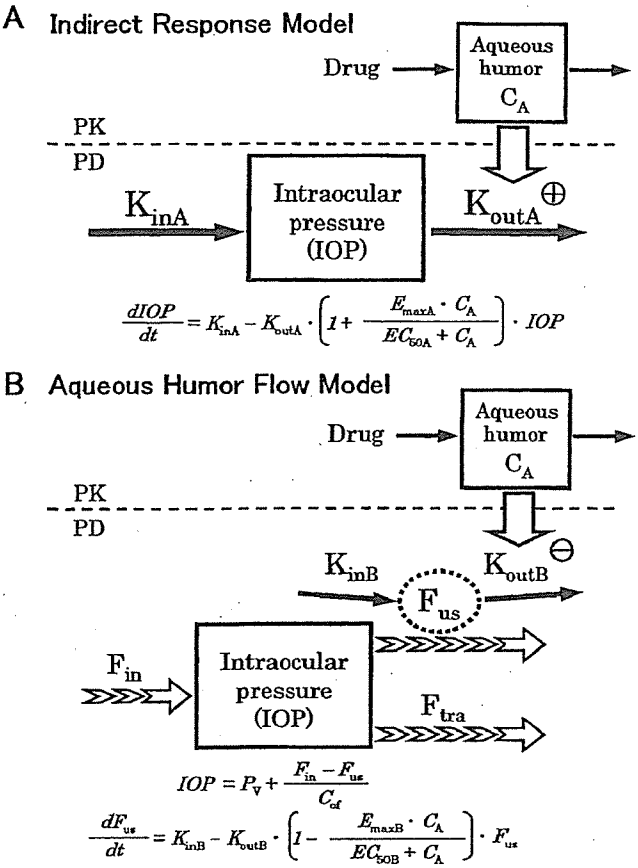

Fig. 6. Pharmacokinetic/pharmacodynamic model for bunazosin: (A) the indirect response model, (B) the aqueous humor flow model.

elimination rate constant and apparent distribution volume were estimated according to a two-compartment model. Figure 2 shows the concentrations of bunazosin in the cornea, aqueous humor, and iris-ciliary body after instillation. The bunazosin concentrations in the cornea were higher than those in the aqueous humor and the iris-ciliary body. The aqueous humor and the iris-ciliary body concentrations of bunazosin reached a maximum at 30 or 60 min after dosing and then gradually disappeared.

The concentration-time profiles of bunazosin in the cornea, aqueous humor, and iris-ciliary body were also determined after injection into the anterior chamber of the rabbits and are shown in Fig. 3. The bunazosin concentrations in the cornea were not much higher than those in the aqueous humor and the iris-ciliary body. The profiles in the aqueous humor and the iris-ciliary body showed a biexponential curve.

In order to develop a PK/PD model for bunazosin, the IOP were determined with a pneumatic tonometer after instillation into the rabbits. Figure 5 shows the hypotensive effect-time profiles of bunazosin after instillation at 0.002%, 0.01%, and 0.1%. The intraocular pressure reductions reached a maximum at 60 min after instillation. Thereafter, the response gradually returned to the baseline with a later return found with the larger dose.

DISCUSSION

Glaucoma is characterized by high IOP, hardening of the eyeball, and partial or complete loss of vision (1). The IOP is maintained by a complex and dynamic equilibrium of aqueous humor production and escape. Bunazosin (α_1-blocker) is commercially available as a new antiglaucoma agent. After topical application, bunazosin has been demonstrated to significantly lower IOP in rabbits (7,11), cats (11), and humans (6). We newly developed a PK/PD model for bunazosin, as there have been no such reports, after its instillation into rabbits.

The physiological complexity of the eye leads to a complicated mathematical model with many compartments and pathways of transportation. Various compartment models have already been reported for antiglaucoma agents such as pilocarpine and timolol (1,12,13). Kato and Iwata (14) successfully described ocular absorption of bunazosin with a simple compartment model after its topical instillation into rabbits. In order to develop an ocular PK model for bunazosin, two experiments using both instillation and injection into the anterior chamber were designed to increase the reliability of the pharmacokinetic parameters.

At first, the concentration-time profiles of bunazosin in the ocular tissues were determined after its instillation (Figs. 1 and 2). Based on the results of the biexponential profiles in tear fluid, a two-compartment model was used to describe the disposition of bunazosin in the precorneal area. Second, the concentration-time profiles of bunazosin in the ocular tissues were determined after its injection into the anterior chamber (Fig. 3). Based on the results of the biexponential profiles in the aqueous humor and the iris-ciliary body, it is assumed that bunazosin distributed to intraocular tissues such as the lens and sclera.

Based on these results, a PK model for bunazosin was established as described in Fig. 4. The PK parameters were estimated according to the model given in Table I. Although the PK model was complicated and had many parameters, the fitting curves using the PK model and the PK parameters almost agreed with the measurements (Figs. 1, 2, and 3).

In order to develop a PK/PD model for bunazosin, IOP was determined with a pneumatic tonometer after its instillation into rabbits (Fig. 5). It was already reported that topical administration of bunazosin significantly reduced IOP in rabbit eyes (7,11). Both single and multiple doses (0.1% × 2 drops) caused a statistically significant decrease in IOP of at least 29% (7), which is comparable with the current study.

Table I. Ocular Pharmacokinetic Parameters for Bunazosin

Parameter	Value	Standard deviation
K_{TR1} (min^{-1})	0.173	0.054
K_{R1T} (min^{-1})	0.118	0.030
K_{Te} (min^{-1})	0.661	0.044
K_{TC} (min^{-1})	0.018	0.002
K_{ES} (min^{-1})	0.212	0.146
$K_{C\Lambda}$ (min^{-1})	0.025	0.004
$K_{\Lambda C}$ (min^{-1})	0.059	0.015
$K_{\Lambda I}$ (min^{-1})	0.141	0.017
$K_{\Lambda R2}$ (min^{-1})	1.267	0.562
$K_{R2\Lambda}$ (min^{-1})	0.359	0.167
$K_{\Lambda e1}$ (min^{-1})	0.010*	
$K_{\Lambda e2}$ (min^{-1})	2×10^{-6}	1×10^{-6}
K_{Ie} (min^{-1})	0.495	0.060

* Value reported by Sakurai *et al.* (4)

Cats and humans were also reported to show a similar IOP reduction (6,11).

In the current study, the relationship between aqueous humor concentrations of bunazosin and IOP changes showed anticlockwise hysteresis, indicating a delayed response. The time for maximal response shifted slightly with dose. Temporal dissociation between the time courses of concentration and effect might be caused by an indirect response mechanism resulting in anticlockwise hysteresis for the concentration-effect (IOP change) relationship (15). Therefore, these results suggest that bunazosin showed a hypotensive effect via an indirect response. Actually, in the preliminary analysis, the hypotensive effect-time profiles of bunazosin showed poor fitting to the common PK/PD (direct response) model (data are not shown). Therefore, we tried to develop the new models.

Indirect Response Model

Many drugs act by inhibiting or stimulating the release of an endogenous substance in nature. These responses via receptors may be considered indirect. Dayneka *et al.* indicated that the actions of adrenergic agonists/antagonists and cholinergic agonists/antagonists could be characterized by the four basic indirect response modelings (8).

The ocular hypotensive mechanism of bunazosin has been investigated in several studies. Bunazosin reportedly is selective for the receptor regulating IOP. In rabbits, it did not affect aqueous flow, but appeared to increase uveoscleral outflow (7). Therefore, in indirect response modeling, the drug concentration in the aqueous humor (C_A) was linked to the PD parameter for IOP loss (K_{outA}). The PD parameters were estimated according to model A (Fig. 6A) as given in Table II. The fitting curves using the PK/PD model and PD parameters were consistent with the measurements (Fig. 5).

Aqueous Humor Flow Model

IOP is required for an optically efficient glove and is generated by the secretion of aqueous humor. Ciliary processes as a result of active transport of solutes form the aqueous humor over the double-layered ciliary epithelium and, secondary to this, diffusion of water. After entering the anterior chamber via the pupil, the aqueous humor is drained by two different pathways at the iridocorneal chamber angle. Some of the aqueous humor enters Schlemm's canal by way of the trabecular meshwork and then passes via the collector channels into the episcleral veins. As there is no epithelial barrier between the anterior chamber and the ciliary muscle, aqueous humor can pass between the muscle bundles into the supraciliary and suprachoroidal spaces, from which it is drained through the sclera. These outflow routes are called the uveoscleral outflow routes (10).

On the other hand, it was reported that IOP is described by an equation including episcleral venous pressure (P_V), aqueous humor flow (F_{in}), uveoscleral outflow (F_{us}), and outflow facility (C_{of}) (10). Antiglaucoma agents change the IOP by influencing the inflow and outflow rates of aqueous humor. Zhan *et al.* reported that bunazosin is an effective ocular hypotensive drug capable of lowering IOP by increasing uveoscleral outflow alone (7). Effects of bunazosin on outflow facility in rabbits have not been reported. Therefore, this PK/PD model considering the relationship between IOP and aqueous humor flow was newly developed to assess the hypotensive effect of bunazosin using physiological parameters (model B, Fig. 6B). In this model, bunazosin indirectly induces uveoscleral outflow by suppressing the receptor (11). The PD parameters were estimated according to model B (Fig. 6B) as given in Table II. The fitting curves using this PK/PD model and PD parameters were consistent with the measurements (Fig. 5). The PK/PD model considering the relationship between IOP and aqueous humor flow (model B, Fig. 6B) showed 73% and 0.002 nmol/ml of E_{maxB} and EC_{50B}, respectively. Kimoto *et al.* reported that the receptor dissociation constant (K_d) of bunazosin was 0.0041 nmol/ml with smooth muscles in the rabbit proximal urethra (16). This K_d value almost agreed with the present EC_{50B} value. Using this K_d for bunazosin on the α_1-receptor, the receptor occupancy values of bunazosin 1 h after instillation of 0.002%, 0.01%, and 0.1% were 60.9%, 88.6%, and 98.7%, respectively (17). A receptor occupancy model can be introduced from the PK/PD model using K_d instead of EC_{50B}. This PK/PD model will be effective in estimating an appropriate regimen for ophthalmic pharmacotherapy and development of ocular drug delivery systems.

The equation for the indirect response model is almost compatible with that of the aqueous humor flow model. Therefore, Akaike's information criteria (AIC) value of the indirect response model (AIC = −5.7) was similar to that of the aqueous humor flow model (AIC = −4.0). Although the indirect response model is a simplified model, the aqueous humor flow model is complicated. The aqueous humor flow model, however, can analyze the physiological behavior of aqueous humor flow after drug administration.

In conclusion, the PK/PD models well described the concentration of bunazosin in the ocular tissues and its hypotensive effect after instillation into rabbits. This study is the first to develop a PK/PD model for an antiglaucoma agent using an indirect response model and the idea of aqueous humor flow.

Table II. Ocular Pharmacodynamic Parameters for Bunazosin

Parameter	Value	Standard deviation
PD parameters		
Indirect response model		
$K_{in\Lambda}$ (mmHg · min^{-1})	0.845*	
$K_{out\Lambda}$ (min^{-1})	0.039	0.037
$E_{max\Lambda}$	0.478	0.177
$EC_{50\Lambda}$ (nmol/ml)	0.014	0.014
Aqueous humor flow model		
K_{inB} (μl/min · min^{-1})	0.077	0.068
K_{outB} (min^{-1})	0.155	0.175
E_{maxB}	0.727	0.170
EC_{50B} (nmol/ml)	0.002	0.003
Physiological parameters†		
F_{in} (μl/min)	2.80	
C_{of} (μl · min^{-1} · mmHg^{-1})	0.170	
P_V (mmHg)	9.00	

* $K_{in\Lambda}$ was estimated by $K_{out\Lambda}$.
† Values reported by Sakurai *et al.* (4).

ACKNOWLEDGMENTS

The author wishes to thank Dr. Yamaoka for supplying MULTI (RUNGE).

REFERENCES

1. H. Sasaki, K. Yamamura, T. Mukai, K. Nishida, J. Nakamura, M. Nakashima, and M. Ichikawa. Enhancement of ocular drug penetration. *Crit. Rev. Ther. Drug Carrier Syst.* **16**:85–146 (1999).
2. K. Yamamura, H. Sasaki, M. Nakashima, M. Ichikawa, T. Mukai, and K. Nishida. and J. Nakamura. Characterization of ocular pharmacokinetics of beta-blockers using a diffusion model after instillation. *Pharm. Res.* **16**:1596–1601 (1999).
3. K. Yamaoka, Y. Tanigawara, T. Nakagawa, and T. Uno. A pharmacokinetic analysis program (MULTI) for microcomputer. *J. Pharmacobiodyn.* **4**:879–885 (1981).
4. M. Sakurai, M. Araie, T. Oshika, M. Mori, N. Shoji, and K. Masuda. Effects of topical application of UF-021, a novel prostaglandin-related compound, on aqueous humor dynamics in rabbit. *Jpn. J. Ophthalmol.* **37**:252–258 (1993).
5. K. Yamaoka and T. Nakagawa. A nonlinear least squares program based on differential equations, MULTI (RUNGE), for microcomputers. *J. Pharmacobiodyn.* **6**:595–606 (1983).
6. T. Takagi, N. Sun, Y. Kuwayama, R. Yamamoto, M. Tanaka, T. Kusunoki, Y. Shimizu, and R. Manabe. The effect of bunazosin hydrochloride on intraocular pressure and aqueous humor dynamics in human. *Acta Soc. Ophthalmol. Jpn.* **95**:273–278 (1991).
7. G. L. Zhan, C. B. Toris, C. B. Camras, Y. L. Wang, and M. E. Yablonski. Bunazosin reduces intraocular pressure in rabbits by increasing uveoscleral outflow. *J. Ocul. Pharmacol. Ther.* **14**:217–228 (1998).
8. N. L. Dayneka, V. Garg, and W. J. Jusko. Comparison of four basic models of indirect pharmacodynamic responses. *J. Pharmacokinet. Biopharm.* **21**:457–478 (1993).
9. J. M. Conrad and J. R. Robinson. Aqueous chamber drug distribution volume measurement in rabbits. *J. Pharm. Sci.* **66**:219–224 (1977).
10. S. F. Nilsson. The uveoscleral outflow routes. *Eye* **11**:149–154 (1997).
11. K. Nishimura, E. Shirasawa, M. Kinoshita, M. Hikida, and Y. Kuwayama. Ocular hypotensive effects of topically applied bunazosin, an α_1-adrenoceptor blocker, in rabbits and cats. *Acta Soc. Ophthalmol. Jpn.* **95**:746–751 (1991).
12. M. C. Makoid and J. R. Robinson. Pharmacokinetics of topically applied pilocarpine in the albino rabbit eye. *J. Pharm. Sci.* **68**: 435–443 (1979).
13. R. D. Schoenwald. Ocular drug delivery. Pharmacokinetic considerations. *Clin. Pharmacokinet.* **18**:255–269 (1990).
14. A. Kato and S. Iwata. Corneal permeability to bunazosin in rabbits. *J. Pharmacobiodyn.* **11**:181–185 (1988).
15. H. Derendorf and B. Meibohm. Modeling of pharmacokinetic/pharmacodynamic (PK/PD) relationships: concepts and perspectives. *Pharm. Res.* **16**:176–185 (1999).
16. Y. Kimoto, M. Nozaki, and T. Itoh. Actions of the alpha-1 adrenoceptor blocker bunazosin on the norepinephrine-induced contraction of smooth muscles in the rabbit proximal urethra. *J. Pharmacol. Exp. Ther.* **241**:1017–1022 (1987).
17. Y. Yamada, K. Matsuyama, K. Ito, Y. Sawada, and T. Iga. Risk assessment of adverse pulmonary effects induced by adrenaline beta-receptor antagonists and rational drug dosage regimen based on receptor occupancy. *J. Pharmacokinet. Biopharm.* **23**: 463–478 (1995).